Computers and Electronics in Agriculture 187 (2021) 106281

Contents lists available at ScienceDirect

Computers and Electronics in Agriculture

journal homepage: www.elsevier.com/locate/compag

Original papers

Mapping tillage direction and contour farming by object-based analysis of UAV images

Francisco Lima [a], Rafael Blanco-Sepúlveda [a], María L. Gómez-Moreno [a], José Dorado [b], José M. Peña [b,*]

[a] Geographic Analysis Research Group, Department of Geography, University of Malaga, Campus of Teatinos, s/n, 29071 Malaga, Spain
[b] Plant Protection Department, Institute of Agricultural Sciences (ICA), Spanish National Research Council (CSIC), C/ Serrano 115-B, 28006 Madrid, Spain

ARTICLE INFO

Keywords:
OBIA4tillage
Soil erosion risk
Good agricultural and environmental conditions
Unmanned aerial vehicle (UAV)
Object-based image analysis (OBIA)
Olive orchards

ABSTRACT

Tillage is a primary agricultural task that causes progressive soil movement and, consequently, severe erosion in sloping farmland, with a high impact on crop productivity, soil quality and landscape features. Governments and public administrations acknowledge the need to control tillage operations for a better soil conservation in vulnerable areas, recommending the practice of contour farming. Despite this importance, there is currently no mechanism for the effective and large-scale monitoring of tillage patterns at the field or regional scale. Accordingly, this research combined aerial images taken with unmanned aerial vehicles and object-based image analysis (OBIA) to develop an innovative *OBIA4tillage* procedure with three main objectives: (i) analysing plowed agricultural fields, identifying and mapping the tillage marks, and automatically computing the main direction of the tillage furrows, (ii) validating the procedure quality in different scenarios by evaluating the accuracy of the results as affected by the sensor used (visible-light *vs*. multispectral), background soil hue, and ground vegetation density; and (iii) mapping contour farming and non-contour farming areas as indicators of potential low and high soil erosion risk, respectively. Twenty olive parcels from two different locations with a wide range of tree sizes, soil hue, parcel shapes and land slopes were selected as model systems to develop and validate the procedure. The *OBIA4tillage* procedure produced tillage maps with very high accuracy for both RGB and multispectral images (R^2 of 0.99 and 0.93, respectively), as obtained from the linear equation between estimated and ground-truth values. The results were similar in clear and dark soils (R^2 of 0.96 in both cases), although there were notable differences between areas of dense ground vegetation or bare soil (R^2 of 0.99 in both cases) and areas of medium vegetation cover (R^2 of 0.81). The application of contour farming in the study region was moderate at location 1 (42.35% of the study area) but more widespread at location 2 (72.60% of the study area), which revealed the uneven involvement of the local farmers in the challenge of controlling soil erosion risks. The valuable information in the *OBIA4tillage* outputs can also be used to study tillage events at various spatial and temporal scales, feed soil erosion models and promote good agricultural and environmental conditions measures implemented at the parcel scale.

1. Introduction

Tillage is a soil management practice that reduces production costs by facilitating various cropping tasks such as seeding, planting, fertilization and weed control; therefore, it remains one of the most common agricultural tasks worldwide (Kienzle et al., 2013). Against these advantages, unreasonable tillage presents a major environmental problem by accelerating erosion processes, being especially dangerous in sloping farmland (Beniston et al., 2015). Tillage erosion is triggered during the production process and sometimes also acts as an aggravating factor for other land erosion events (Wang et al., 2016). Mechanized tillage generates alternative upward and downward soil movements that cause the alteration of the soil structure and make the soil more susceptible to degradation and fertility loss (Zhang et al., 2017). In this sense, tillage direction is a decisive factor for assessing the impact of plowing on the soil profile (Heckrath et al., 2006), together with terrain features such as the slope gradient (Zhang et al., 2019) and other aspects inherent to agricultural practices such as the type of tools used, operation speed and

* Corresponding author.
E-mail address: jmpena@ica.csic.es (J.M. Peña).

https://doi.org/10.1016/j.compag.2021.106281
Received 26 December 2020; Received in revised form 8 June 2021; Accepted 15 June 2021

depth of tillage (Xu et al., 2019). In addition, tillage direction is a critical value to determine input variables in models that study tillage erosion and water soil erosion, such as the tillage transport coefficient and support practice factor (Panagos et al., 2015; Van Oost et al., 2006). The reason for this is that tillage oriented along the land slope can generate preferential runoff paths and cause an increase in water erosion (Souchere et al., 1998). In contrast, contour farming, defined as plowing to constant elevations that are perpendicular to the normal flow direction of runoff (European Commission, 2020), would allow us to control the harmful impacts of tillage on land modification and is considered a soil conservation practice (Panagos et al., 2020). Therefore, the quality of the results provided by these soil erosion models depends largely on determining the tillage direction values and, as a result, defining the contour farming area with higher accuracy, which is viewed with great uncertainty due to the lack of precise and robust methodologies designed for this purpose (Beven and Brazier, 2011; Panagos et al., 2020; Rawat et al., 2016).

Remote sensing is a versatile technology with multiple applications in agricultural and environmental scenarios (Weiss et al., 2020), such as those aimed at monitoring tillage or soil conservation practices (Daughtry et al., 2006; Eskandari et al., 2016; Quemada et al., 2018; South et al., 2004; Zheng et al., 2014), soil erosion phenomena associated with agricultural land uses (Panagos et al., 2014) and natural or artificial landscape features, e.g., terraces and physical obstacles, which allow control of run-off (Karydas et al., 2009). Research specifically focused on the characterization and mapping of tillage metrics is further supported by geographic information systems (GIS), although real implementation of the proposed procedures presents certain limitations because they rely on strict hypotheses or have a very local scope. For example, Drzewiecki (2008) used available digital (aerial or satellite images) spatial data and a GIS environment to define parcel boundaries and applied a criterion of perpendicular coincidence between the main directions of the longest parcel edge and slope aspect to identify the parcels with contour farming in an upland area in southern Poland. This procedure was later automated for application to larger regions through the application of object-based image analysis (OBIA) (Drzewiecki et al., 2014) and implemented in a diversity of soil types and landforms by using light detection and ranging (LIDAR) data and GIS tools (Bozek et al., 2016). This method is valid only under the assumption that the plots are cultivated along their longest edge, which is not necessarily true in the case of mechanized plowing, and prevents its application in square plots with all edges of similar length (Bozek et al., 2016). By applying other criteria, Panagos et al. (2015) estimated contour farming areas at the European level using the 25 m resolution digital elevation model (DEM) and assuming that farmers had correctly implemented the good agricultural and environmental conditions (GAEC) defined in the common agricultural policy aiming to achieve sustainable agriculture (European Union, 2009). However, this approach has the weakness of ignoring the fact that the effective control and monitoring of GAEC compliance is often hampered by technical and methodological problems (Lima et al., 2019).

Despite the cited research efforts, to date, there are no remote sensing applications to accurately assess critical tillage features such as tillage direction and contour farming in cultivated plots, mainly due to the constraints inherent to the spatial resolution of piloted aircraft and satellite images (in the range of many centimetres and a few metres of ground sampling distance (GSD), respectively) that prevent the clear observation of the narrow tillage marks caused by machinery. Alternatively, unmanned aerial vehicles (UAVs) or drones now offer a viable option that has not yet been explored for this purpose. UAVs capture ultrahigh spatial resolution (UHR) and on-demand aerial images (less than 10 cm of GSD) that allow the detection of small geometrical patterns in the terrain, which is not possible with images from other conventional remotely-sensed platforms (Torres-Sánchez et al., 2014, Colomina and Molina, 2014). The main difficulty with these UHR images in complex agricultural scenarios lies in the development of efficient analysis algorithms with the capability to identify tillage features and determine their main metrics. Tillage labour generally follows a fluctuating trajectory depending on parcel orography and the farmer's arbitrary decisions on the time and manner of tilling, and the tillage marks appear in the images as linear objects that are affected by other elements of the scene, such as trees, shadows, cover crops, weeds, stones, etc., which break their linear structure and greatly complicate the image classification processes. This image analysis challenge can be met with the OBIA paradigm, which offers tools that are not available in traditional pixel-based methods (Blaschke et al., 2014). OBIA integrates the spectral, morphological, contextual and hierarchical characteristics of the segmented objects into the analysis, which leads to a high level of robustness and automation and a significant improvement in results compared with pixel-based methods (Castillejo-González et al., 2009; de Castro et al., 2018).

Given the importance of characterizing the tillage events that impact on soil conservation in sloping farmland, this research introduces an innovative OBIA procedure, named *OBIA4tillage*, for the analysis of UAV images of plowed agricultural fields to automatically classify tillage furrows and compute their main direction with very high accuracy and low computational cost. Twenty olive plantations with a wide range of tree sizes, soil hues, parcel shapes and land slopes were selected as model systems to develop and validate the procedure. Specific objectives were to (1) evaluate the performance of the *OBIA4tillage* procedure in remote images of two UAV sensors with different spectral (visible-range and multispectral) and spatial resolutions, (2) determine the impacts of soil hue (clear or dark) and density of ground vegetation in the procedure results, and (3) map contour and non-contour farming areas with the incorporation of the slope aspect layer. Finally, this paper explores the potential of the output tillage direction and contour farming maps to assess the proper implementation of tillage practices in the study region in accordance with the GAEC criteria established to strength sustainable agricultural strategies on sloping farmland.

2. Materials and methods

The full procedure developed in this research is summarized in the following phases (Fig. 1): (1) acquisition of UHR UAV images with two different sensors, (2) generation of geospatial products by applying close-range photogrammetry methods, (3) development and application of the innovative *OBIA4tillage* procedure and generation of grid-based tillage direction maps, (4) evaluation of the results with ground-truth observations, and (5) generation of grid-based contour and non-contour farming maps. Each phase is described in detail in the next sections.

2.1. Study sites and acquisition of the UAV images

The investigation was carried out in 20 commercial olive groves located in two locations in Malaga Province (southern Spain), named Alozaina and Casarabonela (central coordinates 4064214 W, 334494 N and 4068297 W, 336842 N, coordinate system UTM, zone 30 N, datum ETRS89, respectively) (Fig. 2). The region has a temperate Mediterranean climate, with average annual temperature and precipitation of 18.4 °C and 636 mm, respectively. The predominant soils are Calcic Cambisols, Vertic Cambisols, Calcaric Regosols and Haplic Vertisols (FAO and IUSS, 2015) and the landscape is mainly characterized by sloping olive plantations with complex topographic conditions and steep terrain with high gradient variability. Both study locations have average slopes of 10%, with minimun-maximun values of 7–28% and 2–31%, respectively, and their olive trees are non-irrigated and placed in a traditional square plantation pattern at a distance of 8–10 m from each other.

In this agrarian system, farmers apply mechanized tillage two or three times a year mainly to break up the topsoil and improve water infiltration, as well as to remove spontaneous vegetation ground cover.

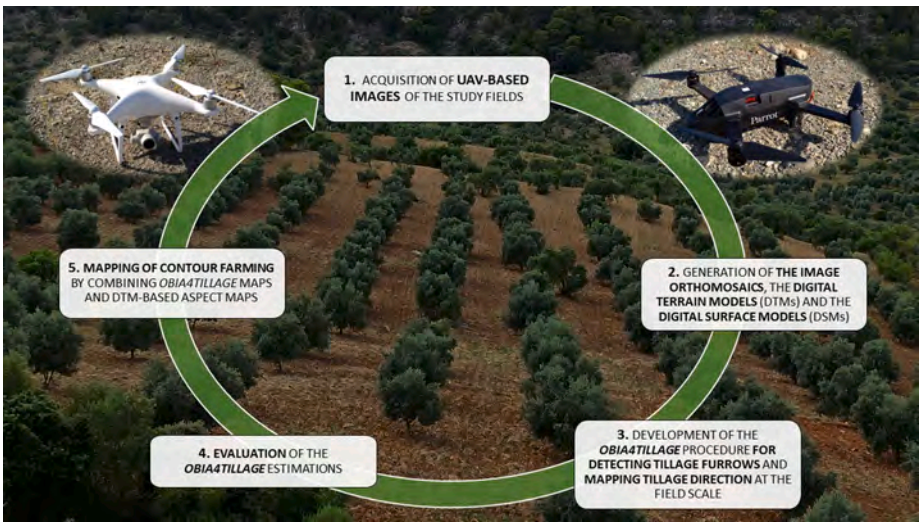

Fig. 1. Flowchart of the main phases carried out in this research.

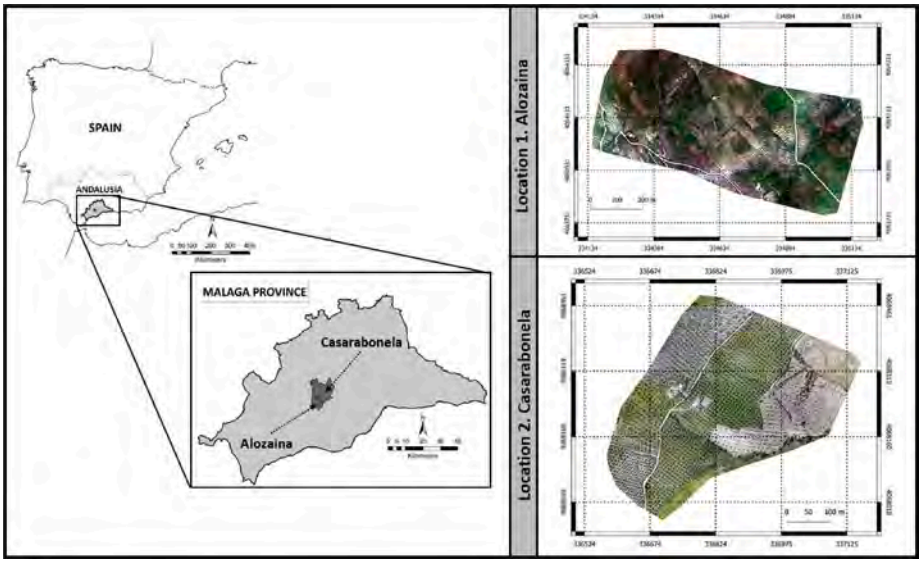

Fig.2. Location map of the study sites in Malaga, Spain (Coordinate system: UTM Zone 30 N, datum ETRS 1989).

The tillage operation usually begins in January after fruit picking and is occasionally repeated until June, and it is carried out using a 2-row and 9-arm cultichisel type tool equipped with duckfoot grids, commonly used in olive groves. As a result, soil is bare for most of the year and has uniform surface forms such as furrows and ridges approximately 15–20 cm deep (Fig. 3).

The aerial images were acquired on April 18, 2018, with two different sensors mounted separately in two UAVs in order to evaluate the capability of the *OBIA4tillage* procedure to monitor the tillage operations in both types of images (Table 1). The flight date was at the end of a tillage period carried out during the previous weeks in the study area; therefore, the superficial marks (furrows and ridges) were relatively recent and still visible both in aerial and on-ground images. Olive growers usually aim to plow generally perpendicular to the land slope (Fig. 3b), although this does not always happen; therefore, tillage direction varies considerably both within and between olive parcels. The images of Alozaina (location 1) were obtained with a Parrot Bluegrass quadcopter and a Parrot Sequoia multispectral sensor (Parrot SA, Paris, France). This sensor is composed of four single-band global shutter cameras with a resolution of 1.2 Mpx (1280 × 960 pixels), capable of capturing four spectral bands in the visible and near-infrared spectral regions, i.e., the green (G), red (R), red edge (RE), and near infrared (NIR) bands. This sensor also records the GPS location, inertial data and the light conditions at each image capture. The images of Casarabonela (location 2) were obtained with a DJI Phantom 4 Pro quadcopter and a 1″ CMOS camera (DJI Ltd., Shenzhen, China). This UAV records the GPS position of each image capture and its camera produces blue (B), G, and R images with a resolution of 20 Mpx (5472 × 3648 pixels). In both cases, the flight altitude was 90 m, and the image overlaps were high enough (30% side-lap and 60% forward-lap) to accurately build the orthomosaics and digital models described in the next stage. The UAV flight routes fulfilled the legal requirements of the Spanish National Agency of Aerial Security and were authorized by a written agreement between the farm owners and our research group.

2.2. Generation of the image orthomosaics and geospatial products (DTM and DSM)

Image mosaicking and generation of the digital terrain and surface models (DTM and DSM, respectively) were performed with Pix4Dmapper Pro software, version 4.2.25 (Pix4D S.A., Prilly, Switzerland), following a sequential process of image aligning, field geometry building

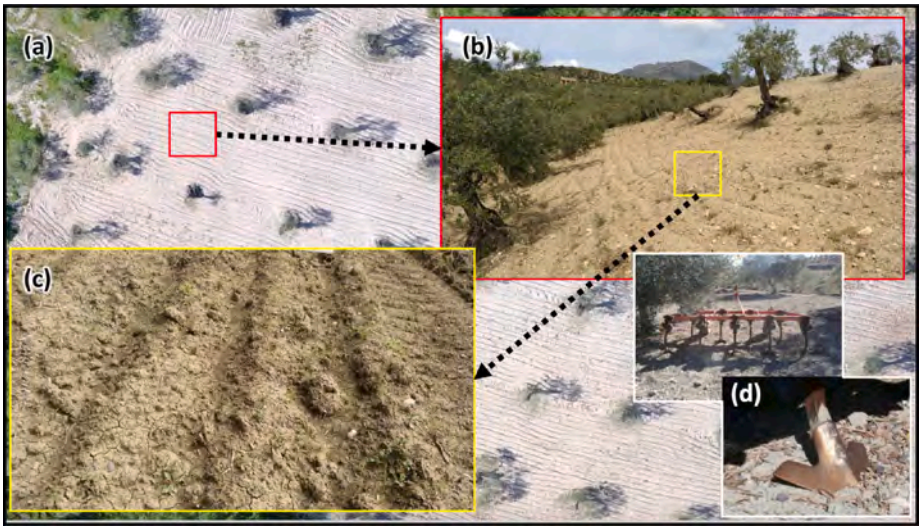

Fig. 3. Signs of tillage observed in UAV aerial images (a) and on-ground views (b, c, d), e.g., contour farming carried out perpendicular to the land slope (b), details of furrow and ridge tillage marks (c), and cultichisel type tool equipped with duckfoot grids (d).

Table 1
Percentage of area with tillage oriented to the north (0–22.5°), northeast (22.5–67.5°), east (67.5–112.5°), southeast (112.5–157.5°) and south (157.5–180°) in the study locations.

	Main orientation of tillage operation (%)				
Location	north	northeast	east	southeast	south
(1) Alozaina	8.97	12.31	27.13	41.90	9.69
(2) Casarabonela	6.46	32.38	27.86	30.63	2.65

and *ortho*-photo generation. The entire process was automatic with the exception of the geolocation of a set of ground control points taken in each study field with a Trimble Geo XH-6000 global position system (GPS) device (Trimble GeoSpatial, Munich, Germany) and produced two orthomosaics with GSD of 0.101 m and 0.037 m and two pairs of DTM/DSM with GSD of 0.50 m and 0.18 m at locations 1 (multispectral image) and 2 (RGB image), respectively. For more information, readers are advised to consult Mesas-Carrascosa et al. (2015).

2.3. The innovative OBIA4tillage procedure for mapping tillage direction

We created an original and innovative algorithm to map tillage operations by using the OBIA paradigm with eCognition Developer 9.5 software (Trimble GeoSpatial, Munich, Germany) and named the entire procedure *OBIA4tillage*, which is structured as a rule-set with several stages. The first and second stages included parcel segmentation and automatic classification of trees, shadows and bare soil, followed by a third stage of identification of tillage furrows and ridges in the bare soil as key elements for computing the tillage direction values. This stage was also designed to disregard lengthwise or linear objects caused by background texture or image noise and not belonging to the tillage marks, thus minimizing the impact of these false positives. Finally, the fourth and fifth stages involved the grid-based mapping of parcels according to tillage direction and the export of data and images. The *OBIA4tillage* algorithm is automatic, robust and self-adaptable to any UHR remote image regardless of the sensor used (RGB or multispectral) and the scenario studied (e.g., tree plantation pattern, soil type, etc.), and it is fully described as follows (Fig. 4):

Stage 1. Image segmentation: Three consecutive segmentation phases were applied to generate a hierarchical structure. The upper level of the hierarchy, named "parcels", was composed of image objects matching the study parcels and was created by applying the vector-based segmentation algorithm with the parcel limits as the reference vector layer (Fig. 5a). The intermediate level, named "grids", was created with the chessboard segmentation algorithm to split the parcel objects into square image objects of a customized size (in this case, 20x20 m) and to create a grid-based framework for site-specific analysis of specific features (i.e., colour, brightness, shape and size) of the sub-objects created below every grid (Fig. 5b). The "parcels" and "grids" segmentation levels were also used for processing the algorithm tasks to smaller scene subsets in separated image domains (object by object), which drastically reduced computing time by focusing the analysis only on the pixels of each object and looping over all objects sequentially. The lower level, named "ground", was created with the multiresolution segmentation algorithm to generate small image objects matching the target elements of the scene, i.e., trees, shadows and tillage signs. This type of segmentation operates on the basis of several parameters defined in this procedure as 20, 0.9, 0.1, 0.5 and 0.5 for scale, colour, shape, smoothness and compactness, respectively, after applying a trial-and-error testing task (Trimble, 2020).

Stage 2. Classification of trees, shadows and bare soil: This stage follows two consecutive steps. The first step was the classification of the tree objects at every parcel level by using a new raster layer obtained as a result of subtracting the DTM from the DSM with the image layer calculator (i.e., DSM-DTM). This new layer was then analysed at the lower "ground" segmentation level and the tree objects were classified after applying a minimum threshold of 0.30 (i.e., corresponding to metres in height), as suggested by Lima et al. (2019). The remaining objects below this threshold corresponded to bare soil, tree shadows, weeds and other ground vegetation, all of which were affected by the tillage operations (Fig. 5c). The second step was masking the tree shadows by calculating the mean brightness of the objects in every 20 × 20 m grid and applying these values as a maximum threshold for shadow classification.

Step 3. Detection of tillage furrows: The image objects belonging to tillage furrows at the "ground" segmentation level were detected by applying a customized operation of two consecutive tasks applied separately to the objects inside every 20x20 m grid. First, a looping process of image object fusion was designed to create new lengthwise objects, in which a seed object was merged with two or more candidate objects only if the length/width (L/W) ratio of the target object increased after merging in comparison to the L/W of the seed object. Second, objects larger than 2 m in length and with an L/W rate higher than 3 were designated tillage furrows (Fig. 5d).

Step 4. Mapping of tillage direction values: The intermediate

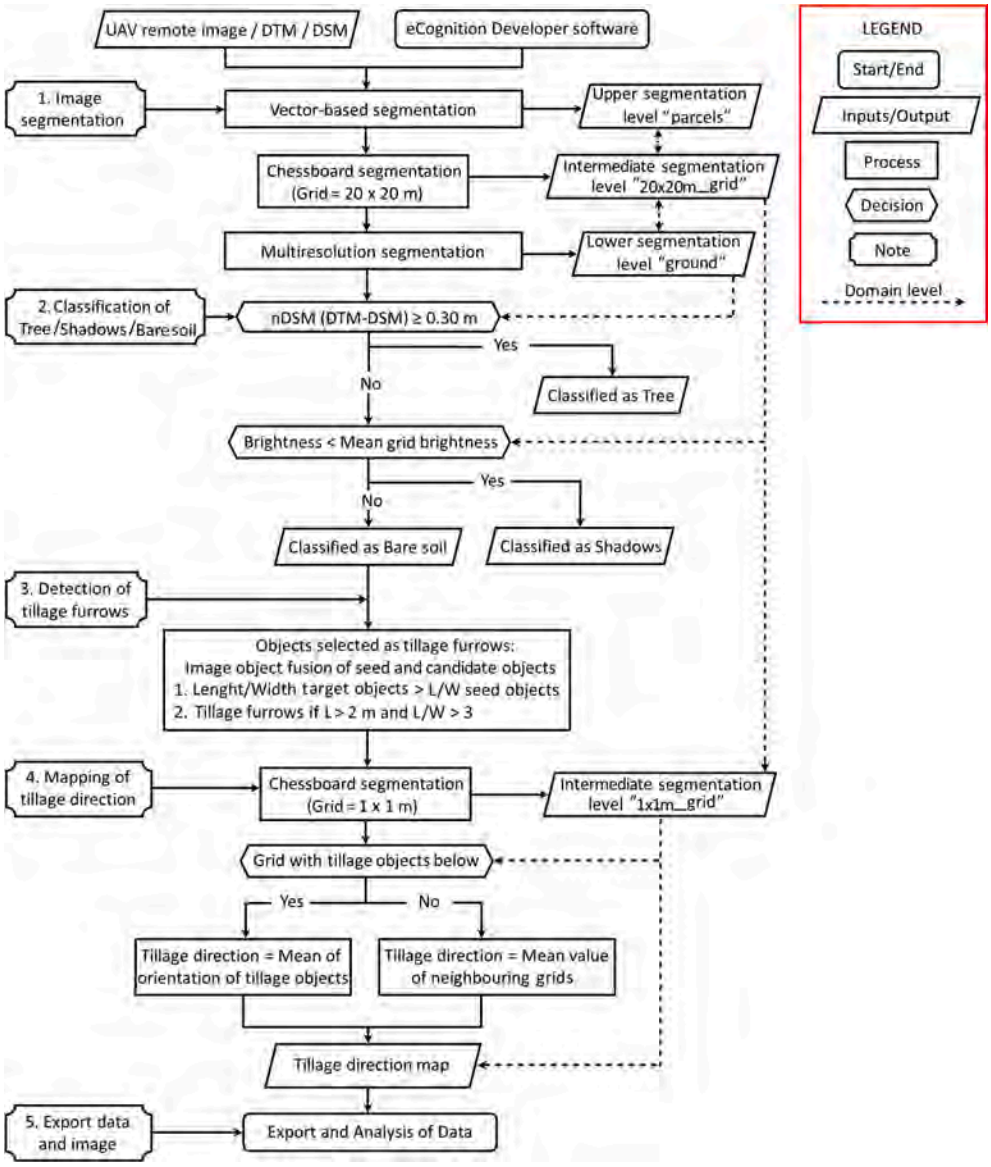

Fig. 4. Flowchart of the OBIA4tillage procedure developed in this investigation for detecting tillage furrows and mapping tillage direction.

segmentation level of 20x20 m grids was divided into smaller grids of 1x1 m with the chessboard segmentation process in order to create a new raster layer with the tillage direction values at a 1 m^2 of spatial resolution, although any other spatial resolution could be also selected according to the useŕs criteria. The mean value of the main direction feature computed from the objects classified as tillage furrows in every 1x1 m grid was assigned as the tillage direction value in the corresponding grids, and thus exploiting the hierarchical relationship between the super-objects at the "1x1 m grid" level and the sub-objects at the "ground" level (Fig. 5e). Those grids that had no sub-objects classified as tillage furrows at the lower level were assigned a tillage direction values averaged from the values of the neighbouring grids, thus exploiting the neighbouring relationship between the objects at the "1x1 m grid" level. The final product was a raster layer with a tillage direction value for every pixel of the image between 0° and 180°, regardless of the land use occupied by the pixel (Fig. 5f).

Step 5. Export data and images: The algorithm outputs were delivered as image (e.g., geoTIFF format), vector (e.g., shapefile format) and table (e.g., ASCII format) files for further analysis and validation of the results with ground-truth observations. The tillage direction maps were also combined with the DTM slope and aspect layers to generate an additional product named the contour farming map, as described in Section 2.5.

2.4. Evaluation of the OBIA4tillage outputs

The *OBIA4tillage* algorithm was created by writing a logical rule-set and using a representative parcel of each location and type of image as training scenarios. Next, the algorithm was applied to the rest of the study region and evaluated in 40 ground-truth validation plots of 10x10 m size from both locations. The validation plots were different from the training fields, resulting in an independent evaluation procedure.

The tillage furrows observed in every validation plot were manually delineated over the orthomosaics and saved as a validation vector file with real values of tillage direction. Next, the validation vectors were overlaid on the tillage direction maps, and the estimated and observed tillage values were compared by calculating the slope, intercept and coefficient of determination (R^2) of the linear equation between both variables. The root mean square error (RMSE) was also calculated as an additional measure of the overall error of the estimations. The *OBIA4-tillage* algorithm was also evaluated according to the type of sensor used, as well as the soil hue (clear *vs*. dark) and ground vegetation density

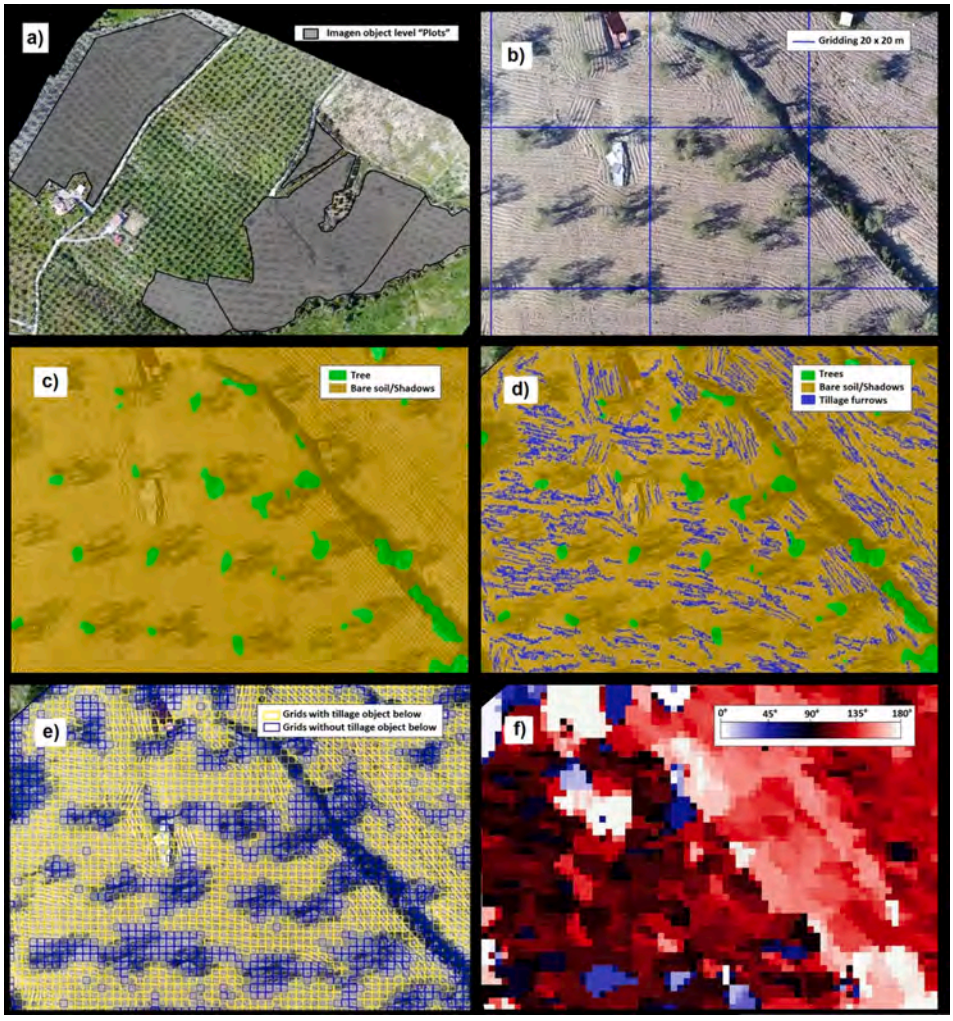

Fig. 5. Partial view of the outputs of the OBIA procedure at each step: (a) vector-based segmentation output at the "parcel" level; (b) chessboard segmentation output at the "20x20 m grid" level; (c) classification of trees, shadows and other ground objects; d) detection of tillage furrows; (e) chessboard segmentation output at the "1 × 1 m grid" level; and (f) mapping of tillage direction values between 0° and 180°.

(bare, sparse, medium and dense) observed in every validation plot.

2.5. Generation of contour farming maps

Contour farming is considered to control the possible negative impacts of tillage operations on soil health by plowing perpendicular to the land slope. Therefore, we combined the layers of tillage direction maps and slope aspect to automatically delineate the contour and non-contour farming areas. The slope aspect layers were calculated from the UAV-based digital terrain models of each study location and using the aspect tool of ArcGIS 10.7 software (ESRI, California, EEUU), and they represent the compass downslope direction of the land slope at each raster cell. The aspect values were measured clockwise in degrees between 0 and 180 (north–south) and 90–270 (east–west) following a full circle. The type of tillage operation in terms of contour (perpendicular to land slope) and non-contour farming (along land slope) were calculated using raster map algebra according to the conservative criteria established by Drzewiecki et al. (2014), who considered contour farming areas if the difference between tillage and aspect directions is in the range of 75 and 105° (i.e., both directions were perpendicular within a range of ±15°), while the non-contour farming areas were the remaining areas (Fig. 6). This threshold can be modified by the user according to the particular conditions of each crop or region, which would logically lead to a different zonation.

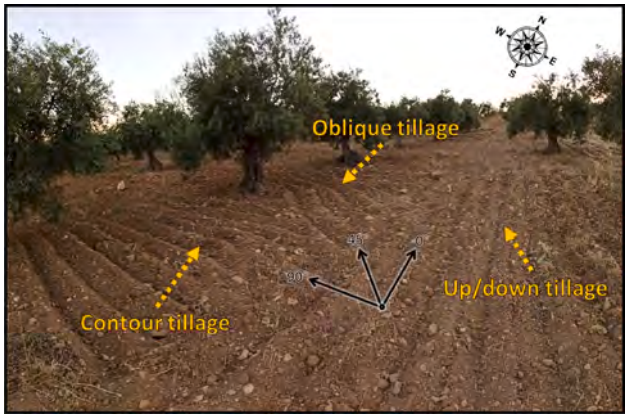

Fig. 6. A field photograph showing different types of tillage operations according to the land slope aspect.

3. Results

3.1. Maps of tillage direction provided by the OBIA4tillage procedure

The main output of the *OBIA4tillage* procedure developed in this

research was grid-based maps with information on the tillage direction at a 1-m of spatial resolution (Fig. 7). These maps served to know the main plowing patterns in each parcel, as well as to identify those singular operations from the main tillage direction that, in most cases, corresponded to common actions such as maneuvers to avoid obstacles, soil tillage next to the trees, and turns after each pass to continue with the work. In addition, the *OBIA4tillage* procedure includes a function to export the map information in table format, allowing descriptive or statistical analysis of tillage operations on a per-parcel, multi-parcel and regional scales. For example, tillage operations in the study area were mainly oriented to the east, southeast and northeast at 81.33% and 90.89% at locations 1 and 2, respectively, while the remaining surface with tillage oriented to north and south was attributed to singular operations (Table 1). The maps and tables obtained in this research allowed us to quantify, with an unprecedented detail, the relative weights of the different maneuvers of soil tillage operations, which are not limited to a single factor but are the result of complex decisions made by the tractor driver based on multiple pieces of information on parcel dimensions and morphology, plantation pattern and land topography.

3.2. Evaluation of the OBIA4tillage procedure

The linear relationship between the observed and estimated values of tillage direction showed a high accuracy of the *OBIA4tillage* procedure in both study locations regardless of the type of sensor used (Fig. 8). The results with the RGB sensor in the parcels of location 2 were slightly better (R2 = 0.992) than those obtained with the multispectral sensor in the parcels of location 1 (R2 = 0.927), with RMSE degree values of 3.23 and 9.65, respectively.

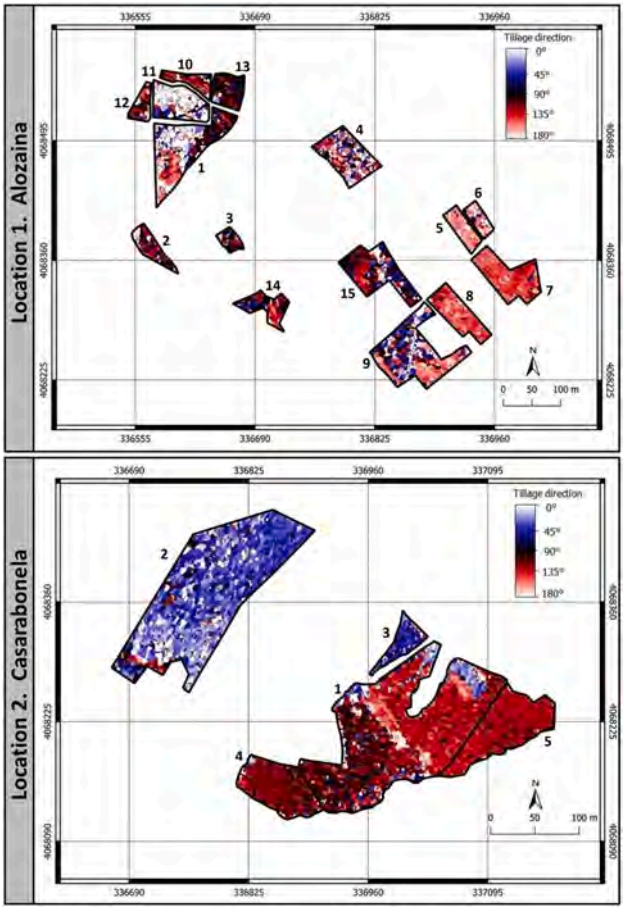

Fig. 7. Maps of tillage direction of the study fields located in Alozaina (location 1) and Casarabonela (location 2).

The other studied variables, such as soil hue and ground vegetation density, had a diverse influence on algorithm performance (Table 2). On the one hand, no differences were observed between clear and dark soils, since similar adjustment metrics were obtained in both cases (R^2 = 0.96), although RMSE was rather better in clear soils. On the other hand, the amount of ground vegetation reported better results with extreme categories (i.e., dense vegetation and bare soil), showing very good linear adjustment between observed and estimated tillage direction values (R^2 = 0.99) and very low RMSE of 2.21 and 3.77, respectively, while accuracy of the algorithm estimations decreased from medium (R^2 = 0.96, RMSE = 6.80) to sparse ground vegetation (R^2 = 0.81, RMSE = 8.20).

3.3. Determining contour farming areas for better soil conservation

The maps of tillage direction (Fig. 7) and maps of slope aspect direction in the range of 0° to 180° (Fig. 9) were combined to generate the contour farming maps (Fig. 10), showing the areas of contour and non-contour farming in every study field. Regarding the slope aspect maps, the parcels in location 1 had hillside orientations in all directions, although the most frequent were the northeast (31.13%) and the north (24.51%). The variability of aspect values in location 2 was lower, clearly predominating on the southeastern (53.45%) and eastern (33.05%) slopes (Table 3). Regarding the tillage operations, the recommended practice of contour farming was not very extensive in location 1, occupying only 42.35% of the total area (Table 4). Of the fifteen study fields, the farmers of only three fields (i.e., numbers 3, 9 and 12) used contour farming in more than 60% of their area, with the farmer of field 12 standing out with more than 90%, thus preventing soil erosion. The rest of the study fields showed a clear predominance of non-contour farming, which was especially harmful to the management of fields 5, 6, 8 and 11, showing more than 80% of their extent under non-contour farming. Land management in location 2 was very different, and contour farming was prevalent, occupying over 70% of the total area. All study fields were plowed with more than 50% of their area under contour farming, with parcels 2 and 3 standing out with more than 95% of their areas preventing soil erosion, while the farmer in field 1 was less careful, tilling almost half of his area with non-contour farming (48.83%).

4. Discussion

The *OBIA4tillage* procedure correctly performed three consecutive tasks: (1) automatic identification of tillage traits, (2) computing the direction of tillage furrows, and (3) zoning the areas of contour and non-contour farming in all study fields. The combination of ultrahigh resolution (UHR) remote images and OBIA techniques was essentially behind the success of these tasks. The furrow and ridge marks generated on the ground by the mechanical tillage tools were clearly visible in the UAV images, and OBIA provided the fundamental algorithms to analyse these marks. In addition to spectral and textural information, the OBIA paradigm also incorporates object geometric features (e.g., extent, shape, etc.), object position features (e.g., absolute or relative coordinates, distances, etc.), and even same-level and hierarchical relationships between objects (i.e., neighbours, sub-objects, and super-objects), which allowed the *OBIA4tillage* procedure to robustly in classify tillage marks and to compute tillage direction values with unprecedented accuracy.

Previous investigations have also exploited the capabilities of remote sensing and OBIA to map linear vegetation/soil features and other singular elements associated with studies of land management practices (Diaz-Varela et al., 2014; Karydas et al., 2009), crop patterns (Peña Barragán et al., 2012; Torres-Sánchez et al., 2015), or agricultural landscapes (Aksoy et al., 2010; Sheeren et al., 2009); but to our knowledge, this is the first attempt to detect and measure the linear

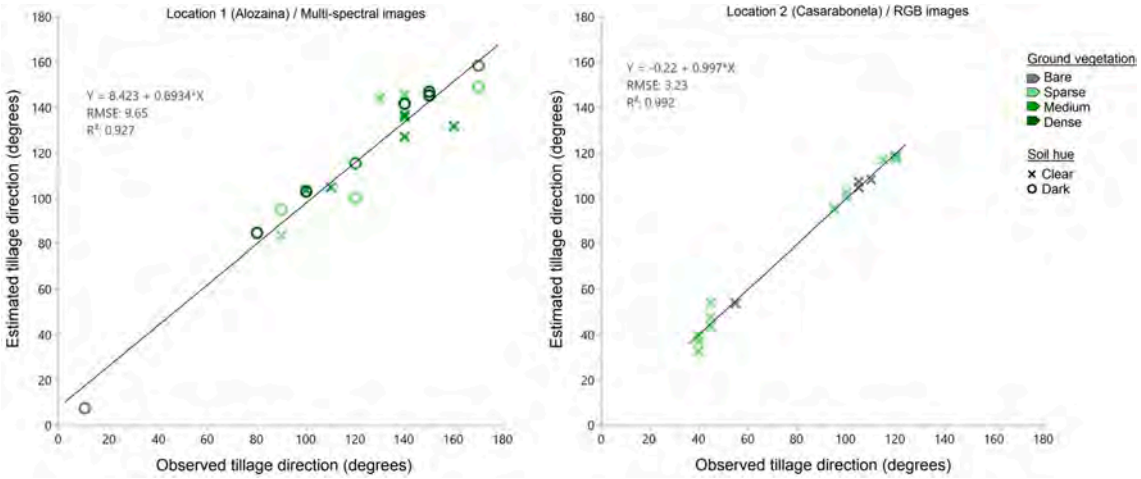

Fig. 8. Observed and estimated values of tillage direction (ranging between 0° and 180°) for the multispectral and RGB orthomosaics collected in Alozaina (location 1) and Casarabonela (location 2), respectively.

Table 2
Linear models between the observed and estimated values of tillage direction according to the type of sensor, soil hue and ground vegetation.

Study variable	Linear model	Prob > F	R^2	RMSE[a]	RMSE for the 1:1 line
Type of sensor					
RGB	Y = −0.22 + 0.99*X	0.0001	0.99	3.23	3.102
Multispectral	Y = 8.42 + 0.89*X	0.0001	0.93	9.65	10.981
Soil hue					
Clear	Y = 3.03 + 0.95*X	0.0001	0.96	7.01	7.198
Dark	Y = 6.05 + 0.91*X	0.0001	0.96	8.43	10.007
Ground vegetation					
Bare	Y = 1.46 + 0.96*X	0.0001	0.99	3.77	4.493
Sparse	Y = 2.58 + 0.95*X	0.0001	0.96	8.20	8.097
Medium	Y = 42.40 + 0.61*X	0.0059	0.81	6.80	12.347
Dense	Y = 13.70 + 0.89*X	0.0001	0.99	2.21	3.579

[a] RMSE: root mean square error

features of tillage operations in cropping scenarios. The cited authors have generally reported superior results over traditional pixel-based approaches, but have also identified some intrinsic weaknesses, such as segmentation errors (Sheeren et al., 2009) or confusion between objects with a similar shape or structure (Aksoy et al., 2010). However, these common errors were overcome in our approach by programming a customized algorithm with a double criterion applied during the phase of automatic detection phase of tillage furrows (Fig. 4). The first criterion was implemented during the task of object fusion, in which the new target objects were only created if they were longer and thinner than the original seed and candidate objects. The second criterion was an extreme domain operation to select the candidate objects with high values of the length and length/width features. The former criterion imposed the generation of longitudinal candidate objects, while the latter criterion ensured that all objects finally classified as tillage furrows truly were tillage marks. A similar customized algorithm has been designed for detecting crop rows with very high accuracy (Peña et al., 2013), although this type of advanced algorithms is rare in the literature regarding OBIA applications in agriculture. OBIA users generally only apply standard segmentation and classification algorithms described by

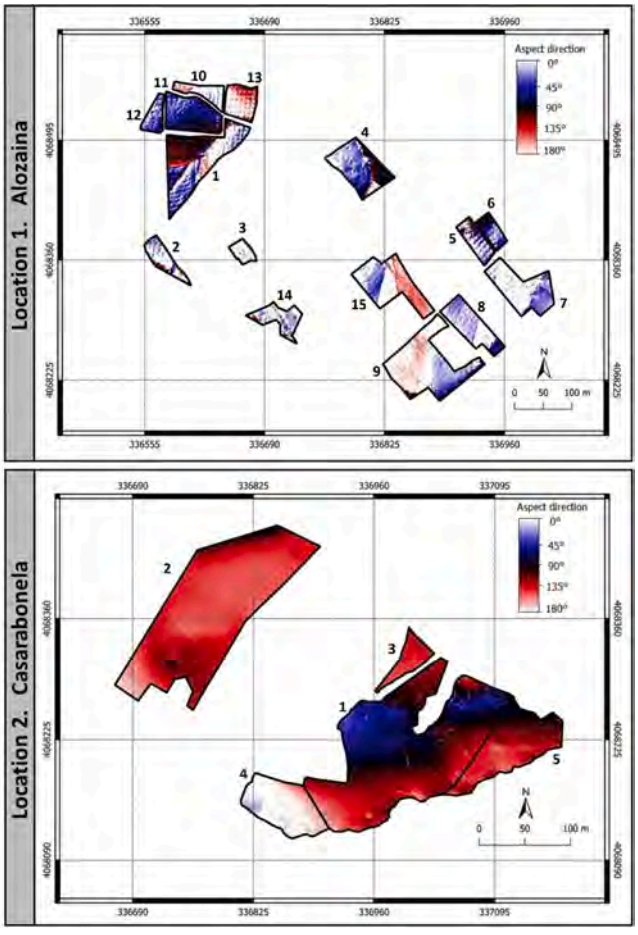

Fig. 9. Maps of slope aspect direction of the fields located in Alozaina (location 1) and in Casarabonela (location 2).

the software guides, and they miss the power of customized algorithms to greatly improve the segmentation outputs and minimize classification errors.

In this research, the *OBIA4tillage* procedure automatically adapted to the intrinsic diversity of the studied fields that had a range of tree sizes, plantation patterns, soil types and densities of on-ground vegetation. This robustness and capacity for autoadaptation by the OBIA rule-set to

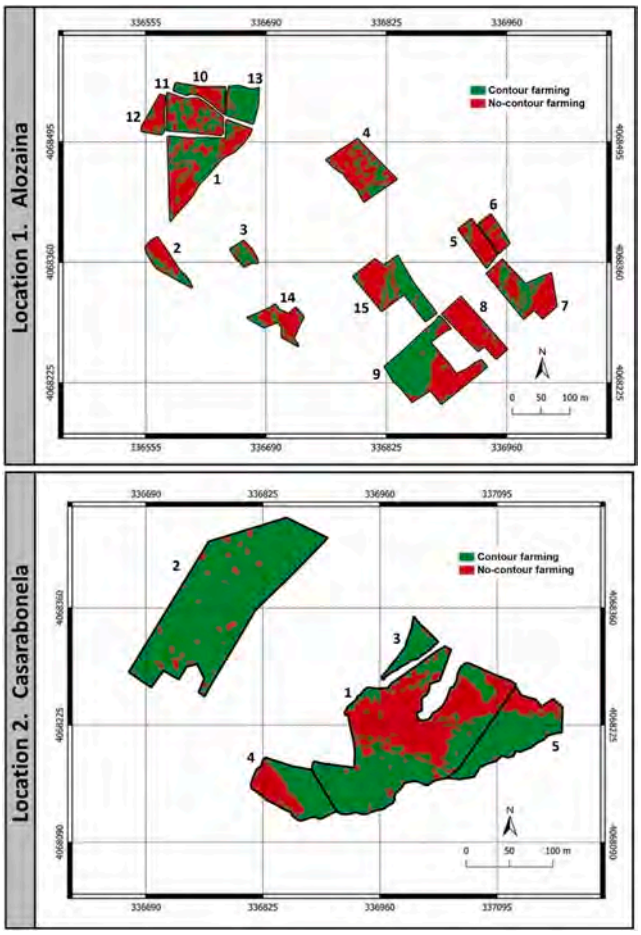

Fig. 10. Maps of contour farming of the fields located in Alozaina (location 1) and in Casarabonela (location 2).

different conditions and scenarios is a remarkable improvement over classic remote sensing methods, where missing information or abrupt alterations in image brightness due to soil colour changes and shadows are common sources of error that seriously impair classification quality and affect the interpretation of results (Ng et al., 2017).

Soil background and vegetation cover were other factors studied in this research, which also often have a high impact on the quality of image analysis (Huete, 1988), mainly in traditional pixel-based classifications. On the one hand, the *OBIA4tillage* procedure was insensitive to soil hue, reporting similar good results for both clear and dark soils ($R^2 = 0.96$). On the other hand, the *OBIA4tillage* procedure reported the best results in areas with extreme values of ground vegetation coverage, i.e., either in zones of dense vegetation or in bare soil (R^2 of 0.99), while it had some imprecision in estimating tillage direction in zones with medium vegetation density (R^2 of 0.81), as the tillage marks were more difficult to identify in these latter scenarios due to the impact of irregular vegetation patches on ground structure. Previous investigations in similar olive grove scenarios have shown that UAV-based multispectral images achieved better estimates of ground vegetation density in cover interval ranges of 10–15% at both high (>80%) and low (<30%) values of vegetation cover and in ranges of 30% at medium vegetation cover values (Lima-Cueto et al., 2019), showing that remote sensing analysis depends on the relative weights of vegetation and soil components in complex agricultural scenarios (Iaquinta and Fouilloux, 1998).

The *OBIA4tillage* procedure was valid to identify the signs of tillage operations with high accuracy in the images collected by both sensors, although the results obtained in the conventional-colour images of the RGB sensor was slightly more precise than the results obtained in the colour-infrared images of the multispectral sensor (R^2 of 0.99 and 0.93, respectively), which can be attributed to the higher spatial resolution of the former (images of 5472 × 3648 pixels, 20 MP) with respect to the latter (images of 1280 × 960 pixels, 1.2 MP). The *OBIA4tillage* procedure did not base its decisions on individual pixels but on groups of adjacent pixels with similar spectral responses that served to define the typical tillage objects (lengthwise or narrow) in the image, regardless of the image type used (conventional-colour or colour-infrared). By comparing the spatial and spectral resolutions of both sensors used, the critical aspect in tillage identification was to have remote images with GSD of a few centimetres, rather than having images with more spectral bands or infrared information, which led to the *OBIA4tillage* procedure to obtain better results with the RGB sensor because its spatial resolution exceeds that of the multispectral sensor.

The *OBIA4tillage* outputs were three georeferenced raster files in GeoTIFF format arranged in a grid of 0.5 m^2 cells containing a value of tillage direction, slope aspect and contour farming (Figs. 7, 9, and 10, respectively), which can also be exported as a vector file in shapefile format and as a tab file in ASCII format for further assessment at intraparcel and interparcel levels (Tables 1, 3, and 4). A complete analysis of these files would allow the user to know the plowing patterns applied by each farmer, to identify the predominant and/or unusual tillage directions and to map the areas where contour farming has or has not been applied according to the land slope, which opens up various topics for discussion. For example, in the study region, a homogeneous pattern with a predominant tillage direction was observed in most parcels, which in many cases did not coincide with the longest side of the parcel, thus contradicting the baseline assumption adopted in previous methods for mapping tillage direction (Drzewiecki et al., 2014). Tillage patterns were different for each parcel due mainly to the personal decision of each farmer, which was based more on economic than environmental criteria. The application of contour farming in the study region was moderate in location 1 (42.35% of the study area) but relevant in location 2 (72.60% of the study area), which revealed an uneven involvement of the local farmers in the challenge of controlling soil erosion risks. According to a farm survey in the study locations, the primary criterion of the local farmers was to reduce the number of tractor maneuvers, which in turn depended on a combination of factors such as the size and shape of the parcels, their topographic characteristics, planting framework and physical obstacles. The shifts in the tillage direction compared with the prevalent route occurred only in very localized areas and mainly in the turns at the end of each pass, when bordering trees and avoiding obstacles or singular elements inside the parcels. This valuable information can be integrated into existing models for tillage translocation that are limited in complex scenarios with numerous trees or obstacles (Vanwalleghem et al., 2010) and can feed the algorithms that predict soil redistribution arising from different patterns of tillage in a given parcel (De Alba, 2003).

Table 3
Slope aspect direction in the study locations.

Location	Slope aspect direction (%)				
	North (0–22.5°)	Northeast (22.5–67.5°)	East (67.5–112.5°)	Southeast (112.5–157.5°)	South (157.5–180°)
1 – Alozaina	24.51	31.13	12.84	12.88	18.62
2 – Casarabonela	3.07	7.23	33.05	53.45	3.17

Table 4
Areas of contour farming reported in each location and parcel of this study.

Location	Parcel ID [a]	Central coordinates[b]		Area (m^2)	Tillage area (%)[c]	
		X	Y		Contour	Non-contour
1 – Alozaina	1	334,263	4,064,362	10,294	45.73	54.27
	2	334,206	4,064,189	2386	31.68	68.37
	3	334,343	4,064,202	1188	67.15	32.85
	4	334,548	4,064,349	6121	30.82	69.18
	5	334,750	4,064,222	2319	14.13	85.87
	6	334,776	4,064,239	1612	17.71	82.29
	7	334,830	4,064,138	6273	35.41	64.59
	8	334,742	4,064,073	4611	4.84	**95.16**
	9	334,665	4,064,004	11,036	60.39	39.61
	10	334,276	4,064,479	5240	47.08	52.92
	11	334,254	4,064,440	1684	17.53	82.47
	12	334,190	4,064,438	2956	**91.74**	8.26
	13	334,340	4,064,463	2863	27.44	72.56
	14	334,406	4,064,085	7043	53.09	46.91
	15	334,601	4,064,146	1959	38.61	61.39
	Total (1)	–	–	67,591	42.35	57.64
2 – Casarabonela	**1**	336,997	4,068,214	21,710	51.17	**48.83**
	2	336,780	4,068,372	19,307	95.86	4.14
	3	336,999	4,068,315	1359	**96.54**	3.46
	4	336,859	4,068,150	4206	60.71	39.29
	5	337,114	4,068,217	5622	78.64	21.36
	Total (2)	–	–	52,205	72.60	27.39
	Total (1 + 2)	–	–	119,796	43.57	56.42

[a] The parcels can be located in Figs. 7, 9 and 10 with their ID.
[b] Coordinate system UTM, Zone 30 N, datum ETRS89.
[c] The fields with the maximum values of tillage and non-contour farming in each location are indicated in bold, while the fields with values above 60% are underlined.

Overall, the *OBIA4tillage* procedure represents a methodological improvement for the study of tillage lands compared with previous research (Bozek et al., 2016; Drzewiecki, 2008; Drzewiecki et al., 2014; Panagos et al., 2020, 2015), and this procedure was proven to be an effective tool to (1) support studies on soil erosion risk assessment, as noted by Rawat et al. (2016), because the tillage direction maps generated with this procedure could serve to refine the estimations of the tillage transport coefficient and the supporting practice factor, and thus contribute to the achievement of an ideal model for estimating soil loss from arable land as argued by Panagos et al. (2020); (2) enable effective and timely control of tillage events through the adoption of a remote sensing system that reports the occurrence of tillage at various spatial and temporal scales (Xu et al., 2019); and (3) provide governments and public agricultural agencies with innovative tools to monitor tillage areas and verify the implementation of GAEC measures related to efficient soil management, such as ensuring compliance with contour farming strategies as stipulated in agricultural regulations such as the European Common Agricultural Policy (European Commission, 2020).

5. Conclusions

This research developed and validated an innovative remote sensing procedure to monitor tillage operations in sloping olive groves and to produce tillage maps with applications in the study of soil erosion events and the follow-up of GAEC measures implemented at parcel scale. The *OBIA4tillage* procedure successfully detected tillage marks and computed the tillage direction values and area of contour farming in complex agricultural scenarios with multiple parcels plowed on various dates and with a range of soil hues, ground vegetation densities, and topographies. This diversity was successfully overcome through the integration of customized algorithms that provided the *OBIA4tillage* procedure with a high degree of automation, along with capacity for autoadaptation and robustness to the real conditions of each parcel.

The *OBIA4tillage* procedure was evaluated with very good results in both conventional-colour and colour-infrared images taken by the RGB and multispectral sensors, respectively, although the results with the RGB sensor were slightly superior to the results with the multispectral sensor. These results were not affected in any sensor by changes in soil hue, although the high accuracies slightly decreased from scenarios with dense vegetation or bare soil to sparse vegetation cover and to a greater extent in areas with medium vegetation density.

One challenge of remote sensing is to serve as an effective technology for assessing the impact of agricultural activities in risky situations concerning soil and environmental conservation, and the procedure presented here represents a significant advance in this regard with the capability to (a) improve the knowledge of the tillage strategies applied by local farmers and the detection of conservation practices such as contour farming and (b) provide precise and timely data on tillage events at various spatial and temporal scales and thus contribute to the information required by soil erosion models.

The *OBIA4tillage* procedure is an efficient tool to monitor tillage practices with unprecedented accuracy and reliability, although future research is needed to evaluate this approach in diverse remote sensing systems (e.g., with images from other UAV-based cameras and sensors, or even satellite platforms) and arable land scenarios (new crops, other types of tillage, diverse landscapes, etc.), as well as to adapt the algorithms to other programming languages or computing platforms (e.g., open-source Python, Google Earth Engine) to increase their scope and applicability to other agricultural regions worldwide.

Declaration of Competing Interest

The authors declare that they have no known competing financial interests or personal relationships that could have appeared to influence the work reported in this paper.

Acknowledgments

This study was conducted within the framework of a predoctoral contract (A.2) under the Research and Transfer Plan of the University of Málaga, and it was also funded by the University of Málaga through the mode B3 of assistance for research projects. The research of Dr. Dorado

and Dr. Peña was financed by the AGL2017-83325-C4-1R project (Spanish Ministry of Science, Innovation and Universities and AEI/EU-FEDER funds). This work also represents a contribution to the CSIC Thematic Interdisciplinary Platform PTI TELEDETECT (https://pti-teledetect.csic.es/). The authors thanks the farmers of the lower Guadalhorce Valley-Sierra de las Nieves and the company TYC-GIS Soluciones Integrales (http://tycgis.com/) for their invaluable cooperation.

References

Aksoy, S., Akcay, H.G., Wassenaar, T., 2010. Automatic mapping of linear woody vegetation features in agricultural landscapes using very high resolution imagery. IEEE Trans. Geosci. Remote Sens. 48, 511–522. https://doi.org/10.1109/TGRS.2009.2027702.

Beniston, J.W., Shipitalo, M.J., Lal, R., Dayton, E.A., Hopkins, D.W., Jones, F., Joynes, A., Dungait, J.A.J., 2015. Carbon and macronutrient losses during accelerated erosion under different tillage and residue management. Eur. J. Soil Sci. 66, 218–225. https://doi.org/10.1111/ejss.12205.

Beven, K.J., Brazier, R.E., 2011. Dealing with uncertainty in erosion model predictions. In: Handbook of Erosion Modelling. Blackwell Publishing Ltd, pp. 52–79. https://doi.org/10.1002/9781444328455.ch4.

Blaschke, T., Hay, G.J., Kelly, M., Lang, S., Hofmann, P., Addink, E., Queiroz Feitosa, R., van der Meer, F., van der Werff, H., van Coillie, F., Tiede, D., 2014. Geographic object-based image analysis – towards a new paradigm. ISPRS J. Photogramm. Remote Sens. 87, 180–191. https://doi.org/10.1016/j.isprsjprs.2013.09.014.

Bozek, P., Janus, J., Taszakowski, J., Glowacka, A., 2016. Determining consistency of tillage direction with soil erosion protection requirements as the element of decision-making process in planning and applying land consolidation. IOP Conf. Ser.: Earth Environ. Sci. 44, 042024. https://doi.org/10.1088/1755-1315/44/4/042024.

Castillejo-González, I.L., López-Granados, F., García-Ferrer, A., Peña-Barragán, J.M., Jurado-Expósito, M., de la Orden, M.S., González-Audicana, M., 2009. Object- and pixel-based analysis for mapping crops and their agro-environmental associated measures using QuickBird imagery. Comput. Electron. Agric. 68, 207–215. https://doi.org/10.1016/j.compag.2009.06.004.

Colomina, I., Molina, P., 2014. Unmanned aerial systems for photogrammetry and remote sensing: a review. ISPRS J. Photogramm. Remote Sens. 92, 79–97. https://doi.org/10.1016/j.isprsjprs.2014.02.013.

Daughtry, C.S.T., Doraiswamy, P.C., Hunt Jr., Stern, A.J., McMurtrey III, J.E., Prueger, J. H., 2006. Remote sensing of crop residue cover and soil tillage intensity. Soil Tillage Res. 91, 101–108. https://doi.org/10.1016/j.still.2005.11.013.

De Alba, S., 2003. Simulating long-term soil redistribution generated by different patterns of mouldboard plowing in landscapes of complex topography. Soil Tillage Res. 71, 71–86. https://doi.org/10.1016/S0167-1987(03)00042-4.

de Castro, A.I., Six, J., Plant, R.E., Peña, J.M., 2018. Mapping crop calendar events and phenology-related metrics at the parcel level by object-based image analysis (OBIA) of MODIS-NDVI time-series: a case study in Central California. Remote Sens. 10, 1745. https://doi.org/10.3390/rs10111745.

Diaz-Varela, R.A., Zarco-Tejada, P.J., Angileri, V., Loudjani, P., 2014. Automatic identification of agricultural terraces through object-oriented analysis of very high resolution DSMs and multispectral imagery obtained from an unmanned aerial vehicle. J. Environ. Manage. 134, 117–126. https://doi.org/10.1016/j.jenvman.2014.01.006.

Drzewiecki, W., 2008. Sustainable land-use planning support by GIS-based evaluation of landscape functions and potentials. In: The International Archives of the Photogrammetry, Remote Sensing and Spatial Information Sciences, Part B7. Beijing, China.

Drzewiecki, W., Wężyk, P., Pierzchalski, M., Szafrańska, B., 2014. Quantitative and qualitative assessment of soil erosion risk in Małopolska (Poland), supported by an object-based analysis of high-resolution satellite images. Pure Appl. Geophys. 171, 867–895. https://doi.org/10.1007/s00024-013-0669-7.

European Commission, 2020. CAP specific objectives... explained – Brief no 5: efficient soil management. Available online: https://ec.europa.eu/info/sites/info/files/food-farming-fisheries/key_policies/documents/cap-specific-objectives-brief-5-soil_en.pdf (accessed on 18 June 2021).

Eskandari, I., Navid, H., Rangzan, K., 2016. Evaluating spectral indices for determining conservation and conventional tillage systems in a vetch-wheat rotation. Int. Soil Water Conserv. Res. 4, 93–98. https://doi.org/10.1016/j.iswcr.2016.04.002.

European Union, 2009. Council Regulation (EC) No 73/2009 of 19 January 2009 establishing common rules for direct support schemes for farmers under the common agricultural policy and establishing certain support schemes for farmers.

FAO and IUSS, 2015. World reference base for soil resources 2014: International soil classification system for naming soils and creating legends for soil maps – Update 2015, World Soil Resources Reports. FAO, Rome, Italy.

Heckrath, G., Halekoh, U., Djurhuus, J., Govers, G., 2006. The effect of tillage direction on soil redistribution by mouldboard plowing on complex slopes. Soil Tillage Res. 88, 225–241. https://doi.org/10.1016/j.still.2005.06.001.

Huete, A.R., 1988. A soil-adjusted vegetation index (SAVI). Remote Sens. Environ. 25, 295–309. https://doi.org/10.1016/0034-4257(88)90106-X.

Iaquinta, J., Fouilloux, A., 1998. Influence of the heterogeneity and topography of vegetated land surfaces for remote sensing applications. Int. J. Remote Sens. 19, 1711–1723. https://doi.org/10.1080/014311698215207.

Karydas, C.G., Sekuloska, T., Silleos, G.N., 2009. Quantification and site-specification of the support practice factor when mapping soil erosion risk associated with olive plantations in the Mediterranean island of Crete. Environ. Monit. Assess. 149, 19–28. https://doi.org/10.1007/s10661-008-0179-8.

Kienzle, J., Ashburner, J.E., Sims, B.G., 2013. Mechanization for Rural Development: A Review of Patterns and Progress from Around the World. Integrated Crop Management. Food and Agriculture Organization of the United Nations (FAO), Rome, Italy.

Lima, F.J., Blanco-Sepúlveda, R., Gómez-Moreno, M.L., Galacho-Jiménez, F.B., 2019. Using vegetation indices and a UAV imaging platform to quantify the density of vegetation ground cover in olive groves (Olea Europaea L.) in Southern Spain. Remote Sens. 11, 2564. https://doi.org/10.3390/rs11212564.

Lima-Cueto, F.J., Blanco-Sepúlveda, R., Gómez-Moreno, M.L., Galacho-Jiménez, F.B., 2019. Using vegetation indices and a UAV imaging platform to quantify the density of vegetation ground cover in olive groves (Olea Europaea L.) in Southern Spain. Remote Sens. 11, 2564. https://doi.org/10.3390/rs11212564.

Mesas-Carrascosa, F.J., Torres-Sánchez, J., Clavero-Rumbao, I., García-Ferrer, A., Peña, J.-M., Borra-Serrano, I., López-Granados, F., 2015. Assessing optimal flight parameters for generating accurate multispectral orthomosaicks by UAV to support site-specific crop management. Remote Sens. 7, 12793–12814. https://doi.org/10.3390/rs71012793.

Ng, M.K.-P., Yuan, Q., Yan, L., Sun, J., 2017. An adaptive weighted tensor completion method for the recovery of remote sensing images with missing data. IEEE Trans. Geosci. Remote Sens. 55, 3367–3381. https://doi.org/10.1109/TGRS.2017.2670021.

Panagos, P., Ballabio, C., Poesen, J., Lugato, E., Scarpa, S., Montanarella, L., Borrelli, P., 2020. A soil erosion indicator for supporting agricultural, environmental and climate policies in the European union. Remote Sens. 12, 1365. https://doi.org/10.3390/rs12091365.

Panagos, P., Borrelli, P., Meusburger, K., van der Zanden, E.H., Poesen, J., Alewell, C., 2015. Modelling the effect of support practices (P-factor) on the reduction of soil erosion by water at European scale. Environ. Sci. Policy 51, 23–34. https://doi.org/10.1016/j.envsci.2015.03.012.

Panagos, P., Christos, K., Cristiano, B., Ioannis, G., 2014. Seasonal monitoring of soil erosion at regional scale: an application of the G2 model in Crete focusing on agricultural land uses. Int. J. Appl. Earth Obs. Geoinf. 27, 147–155. https://doi.org/10.1016/j.jag.2013.09.012.

Peña Barragán, J.M., Kelly, M., de Castro, A.I., López Granados, F., 2012. Object-based approach for crop row characterization in UAV images for site-specific weed management. In: 4th GEOBIA. Presented at the 4th Geographic Object-Based Image Analysis (GEOBIA) Conference. Rio de Janeiro, Brasil, pp. 426–430.

Peña, J.M., Torres-Sánchez, J., de Castro, A.I., Kelly, M., López-Granados, F., 2013. Weed mapping in early-season maize fields using object-based analysis of unmanned aerial vehicle (UAV) images. PLoS ONE 8, e77151. https://doi.org/10.1371/journal.pone.0077151.

Quemada, M., Hively, W.D., Daughtry, C.S.T., Lamb, B.T., Shermeyer, J., 2018. Improved crop residue cover estimates obtained by coupling spectral indices for residue and moisture. Remote Sens. Environ. 206, 33–44. https://doi.org/10.1016/j.rse.2017.12.012.

Rawat, K.S., Mishra, A.K., Bhattacharyya, R., 2016. Soil erosion risk assessment and spatial mapping using LANDSAT-7 ETM +, RUSLE, and GIS—a case study. Arab J Geosci 9, 1–22. https://doi.org/10.1007/s12517-015-2157-0.

Sheeren, D., Bastin, N., Ouin, A., Ladet, S., Balent, G., Lacombe, J.-P., 2009. Discriminating small wooded elements in rural landscape from aerial photography: a hybrid pixel/object-based analysis approach. Int. J. Remote Sens. 30, 4979–4990. https://doi.org/10.1080/01431160903022928.

Souchere, V., King, D., Daroussin, J., Papy, F., Capillon, A., 1998. Effects of tillage on runoff directions: consequences on runoff contributing area within agricultural catchments. J. Hydrol. 206, 256–267. https://doi.org/10.1016/S0022-1694(98)00103-6.

South, S., Qi, J., Lusch, D.P., 2004. Optimal classification methods for mapping agricultural tillage practices. Remote Sens. Environ. 91, 90–97. https://doi.org/10.1016/j.rse.2004.03.001.

Torres-Sánchez, J., López-Granados, F., Serrano, N., Arquero, O., Peña, J.M., 2015. High-throughput 3-D monitoring of agricultural-tree plantations with unmanned aerial vehicle (UAV) technology. PLoS ONE 10, e0130479. https://doi.org/10.1371/journal.pone.0130479.

Torres-Sánchez, J., Peña, J.M., de Castro, A.I., López-Granados, F., 2014. Multi-temporal mapping of the vegetation fraction in early-season wheat fields using images from UAV. Comput. Electron. Agric. 103, 104–113. https://doi.org/10.1016/j.compag.2014.02.009.

Trimble, 2020. Trimble eCognition Suite. Available online: https://docs.ecognition.com/v10.0.0/ (accessed on 27 April 2021).

Van Oost, K., Govers, G., De Alba, S., Quine, T.A., 2006. Tillage erosion: a review of controlling factors and implications for soil quality. Prog. Phys. Geogr.: Earth Environ. 30, 443–466. https://doi.org/10.1191/0309133306 pp487ra.

Vanwalleghem, T., Jiménez-Hornero, F.J., Giráldez, J.V., Laguna, A., 2010. Simulation of long-term soil redistribution by tillage using a cellular automata model. Earth Surf. Proc. Land. 35, 761–770. https://doi.org/10.1002/esp.1923.

Wang, Y., Zhang, J.H., Zhang, Z.H., Jia, L.Z., 2016. Impact of tillage erosion on water erosion in a hilly landscape. Sci. Total Environ. 551–552, 522–532. https://doi.org/10.1016/j.scitotenv.2016.02.045.

Weiss, M., Jacob, F., Duveiller, G., 2020. Remote sensing for agricultural applications: a meta-review. Remote Sens. Environ. 236, 111402. https://doi.org/10.1016/j.rse.2019.111402.

Xu, H.C., Jia, L.Z., Zhang, J.H., Zhang, Z.H., Wei, Y.H., 2019. Combined effects of tillage direction and slope gradient on soil translocation by hoeing. CATENA 175, 421–429. https://doi.org/10.1016/j.catena.2018.12.039.

Zhang, J., Yang, M., Deng, X., Liu, Z., Zhang, F., 2019. The effects of tillage on sheet erosion on sloping fields in the wind-water erosion crisscross region of the Chinese Loess Plateau. Soil Tillage Res. 187, 235–245. https://doi.org/10.1016/j.still.2018.12.014.

Zhang, J.H., Wang, Y., Jia, L.Z., Zhang, Z.H., 2017. An interaction between vertical and lateral movements of soil constituents by tillage in a steep-slope landscape. CATENA 152, 292–298. https://doi.org/10.1016/j.catena.2017.01.030.

Zheng, B., Campbell, J.B., Serbin, G., Galbraith, J.M., 2014. Remote sensing of crop residue and tillage practices: Present capabilities and future prospects. Soil Tillage Res. 138, 26–34. https://doi.org/10.1016/j.still.2013.12.009.